Hydrophobic Hydration in an Orientational Lattice Model

Nara Guisoni*,† and Vera Bohomoletz Henriques‡,§

Instituto de Pesquisa e Desenvolvimento, Universidade do Vale do Paraíba (UNIVAP), Av. Shishima Hifumi, 2911, Urbanova cep 12244-000, São José dos Campos, SP, Brazil, and Instituto de Física, Universidade de São Paulo, C. P. 66318, cep 05315−970, São Paulo, SP, Brazil

Received: February 3, 2006; In Final Form: June 1, 2006

To shed light on the microscopic mechanism of hydrophobic hydration, we study a simplified lattice model for water solutions in which the orientational nature of hydrogen bonding as well as the degeneracy related to proton distribution are taken into account. Miscibility properties of the model are looked at for both polar (hydrogen bonding) and nonpolar (non-hydrogen bonding) solutes. A quasichemical solution for the pure system is reviewed and extended to include the different kinds of solute. A Monte Carlo study of our model yields a novel feature for the local structure of the hydration layer: energy correlation relaxation times for solvation water are larger than the corresponding relaxation times for bulk water. This result suggests the presence of ordering of water particles in the first hydration shell. A nonassociating model solvent, represented by a lattice gas, presents opposite behavior, indicating that this effect is a result of the directionality of the interaction. In presence of polar solutes, we find an ordered mixed pseudophase at low temperatures, indicating the possibility of closed loops of immiscibility.

1. Introduction

Water exhibits anomalous behavior not only as a pure substance[1] but also as a solvent.[2−4] By increasing temperature, one would expect to increase miscibility as a consequence of increasing entropy. Nevertheless, water displays a minimum in the solubility of nonpolar substances in some region of temperature[2] and may also present a lower critical solution temperature in the case of hydrogen-bonding solutes.[3−5] Such properties have been interpreted to be consequences of the presence of hydration entropy, as suggested some time ago by Frank and Evans.[6] However, water structure is of difficult experimental access and measurements that provide direct evidence of structuring of the solvation shell of nonpolar solutes are scarce and contradictory.[7] An earlier theoretical study[8] shows that water dielectric relaxation rate suffers a slowing down in the presence of hydrophobic solutes, a result that may be interpreted in terms of the slowing down of the rotation of molecules in the hydration layer. Evidence of the latter had been seen in a previous experimental study.[9] More recently, neutron diffraction experiments[10] have been obtained, which according to the authors, are consistent with apolar solutes located in cavities in the HB network, with a very small effect of structure of the apolar hydration shell. The idea of a low entropy solvation shell has been probed in a very large number of simulational studies.[11−15] Nonetheless, evidence has not been considered conclusive.

Hydrogen bonding between two water molecules requires specific orientation of those molecules. Liquid water presents a fluctuating and distorted net of bonds as compared to ice, for which full bonding implies low density. The HB net has large positional degeneracy related to the proton distribution on bonds. These three features of the HB net, namely the orientational interaction, the entropy of the proton distribution, and expansion on bonding, have been explored in different lattice models.

A large number of studies rest on the idea of representing the orientational degrees of freedom of the water molecules through Potts variables.[16,17] Two neighboring particles in a selected Potts state are considered to form a bond, a simplifying assumption with respect to the real case, in which both molecules are not necessarily in the same state. Volume increments under the presence of a bond are added ad hoc. Under such conditions, the expected anomalous thermodynamic properties of water are reproduced qualitatively. Potts models have also been used to study water solubility properties. Widom and collaborators[4,18,19] have explored a model in which Potts ordering favors solubilization and were able to obtain decreasing solubility with temperature.

Reduction of solubility with increasing temperature is also exhibited by a different kind of model in which squares and triangles on a lattice are considered to have an orientational interaction.[20,21] Miscibility gaps and loops or reentrances in the temperature−concentration phase diagram are obtained. However, the later models lack the possibility of presenting an HB net because the solute−solvent orientational interaction is emphasized, while the solvent−solvent orientational interactions are disregarded.

Alternatively, the restriction of a single bonding state may be lifted and the entropy of the hydrogen distribution on the bond net (hydrogen bond donors and acceptors) may be included, as in the square ice model,[22] one of the few soluble lattice models of direct physical interest[23] capable of describing the entropy of ice. From a lattice point of view, the ice rules proposed by Pauling[22] imply that a specific set of pairs of states, depending on relative position, represent a bond, but the two neighboring particles must not necessarily be in the same state. Thus a completely hydrogen-bonded (site) Potts model has null entropy, whereas an ice model has an entropy of ∼ln(1.5) per

* Corresponding author. E-mail: nara@univap.br.
† Instituto de Pesquisa e Desenvolvimento, Universidade do Vale do Paraíba.
‡ Instituto de Física, Universidade de São Paulo.
§ E-mail: vhenriques@if.usp.br.

10.1021/jp060729f CCC: $33.50
Published on Web 08/05/2006

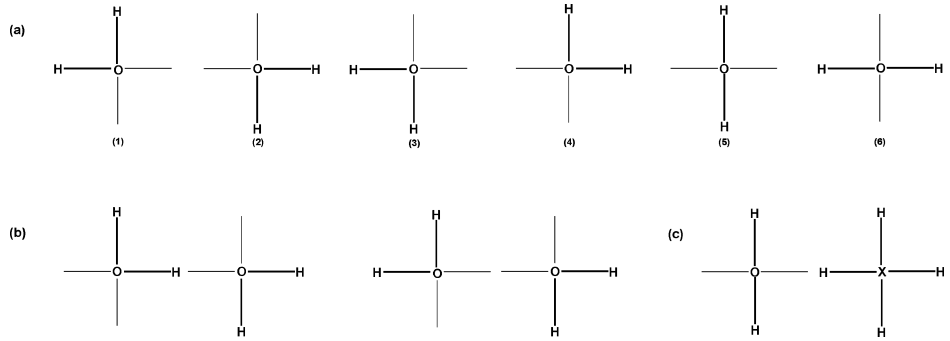

Figure 1. (a) Six states for the water particle. Oxygens are on lattice sites and hydrogens on the edges. (b) An HB is present if there is one hydrogen atom on the lattice line. The first water pair contributes with HB energy $-\epsilon$. Rotation of the left water molecule "breaks" the bond, as in the second pair. (c) The polar solute particle has four hydrogen atoms (on the right). The water−solute HB $-\delta$ is present only if the hydrogen atom of the water molecule does not point to the solute particle.

particle (which is near to the experimental value). The properties of a thermal variant of the ice model, called square water, based on the idea of molecular rotations and "broke" bonds with fixed density, has been studied by different authors.[24−26]

In spite of its simplicity, square water has no analytical solution. As proven by Izmailian and collaborators,[27] square water may be mapped on a nonsymmetric eight-vertex model that lacks an analytical solution.[28] Monte Carlo simulations[24,26] show that the square water model does not exhibit a phase transition related to hydrogen bond ordering, and an independent bond approximation[24] gives a good description of its thermal behavior, a feature which disappears in the presence of solute[26] or under an electric field.[29]

Investigation of thermodynamic anomalies for this model, which could be present if ad hoc liquid density variations were added to bonding, have not been carried out. A variant of square water with allowance for density variations exhibits a negative expansion coefficient.[30,31]

Ice-like variables have also been considered in three-dimensional (3-D) lattice models that allow for density variations,[17,32,33] and corresponding mean-field solutions yield anomalous density properties similar to those of water. Alternatively, some authors have proposed models, both in two and three dimensions, which ignore hydrogen distribution on the bond net, in other words, disregarding the distinction between donor and acceptor arms[34−38] and allowing for density variations. These variants exhibit a density anomaly, as expected. However, the relevance of hydrogen positional entropy on the special properties of water has not yet been clearly established. Solubility properties of related models have been investigated,[38−42] and evidence of hydrophobic hydration has been suggested through analysis of average enthalpy and entropy.

In this paper, we investigate the miscibility properties of square water under fixed density. In a previous short study,[26] we have looked at square water as a solvent for apolar molecules and found that the frequency of hydrogen bonds of the solvation shell is less sensitive to temperature than the frequency of bulk water bonds. In this study, we look further into the properties of the model as solvent, both for polar and nonpolar molecules. Square water, pure and as a solvent, is defined in the following section. Calculations on the Bethe lattice (quasichemical solution) and Monte Carlo results are presented, respectively, in Sections 3 and 4. Discussion and summary of our results are given in Section 5.

2. The Models

2.1. Pure Square Water. Pure square water is a thermal version of the ice model[22] and consists of a square lattice whose points are occupied by oxygens and whose lines[43] are occupied by hydrogens. There are six different states per water particle, related to the possible distribution of two hydrogens on four lattice lines (Figure 1a). The hydrogen bond is present when the hydrogen atom of one molecule (donor) points to the oxygen of a neighbor (acceptor) and is absent when neighboring molecules are both donors or both acceptors on a given line. Typical situations are illustrated in Figure 1b. In the presence of a hydrogen bond (HB), an energy $-\epsilon$ is attributed to the lattice line, otherwise the energy is zero. Because the bond between two neighboring molecules depends on the relative positions of the hydrogen atoms, the model mimics the directional nature of HBs[44] despite the fact that it is a lattice model. van der Waals interactions, usually an order of magnitude smaller than HBs,[45] are ignored.

2.2. Square Water as a Solvent. The properties of a square water solvent are tested in two models for aqueous solutions: (i) of apolar solutes and (ii) of a hydrogen-bonding solute. In both cases, solute particles are single-site.

In the first case, nonpolar molecules, for simplicity, are considered inert (interactions with water or among solutes are disregarded). HBs are allowed to "break" due either to the presence of nonpolar particles or, as in pure square water, as a result of thermal fluctuations.

In the second case, polar solutes are considered hydrogen bonding. They act only as hydrogen donors and thus hydrogen bond only with water particles (each solute can make up to four HBs). Figure 1c illustrates such bonds, which are given an energy $-\delta$. We also consider van der Waals interactions between first nearest neighbors: $-\upsilon_{ww}$, $-\upsilon_{ss}$, and $-\upsilon_{ws}$, where the subindex w (s) indicates a water (solute) molecule.

3. Quasichemical Approximation

Pure square water is a particular case of the general six-vertex model with bond defects[46] discussed by Izmailian et al.[27] The authors show that the general six-vertex model with bond defects may be mapped onto an eight-vertex model in the presence of an electric field and that an exact solution is available only for a very particular situation: in the case where two specific states, among the six possible states, have zero Boltzmann weight (states 1 and 2 or 3 and 4 of Figure 1a). However, for the water model, this condition is not fulfilled and an exact solution is not available, so one has to resort to a Bethe lattice (quasichemical approximation) in order to obtain an analytical solution. We have applied to pure square water a simplified version of the treatment given by Izmailian et al., which we present below, to introduce notation.

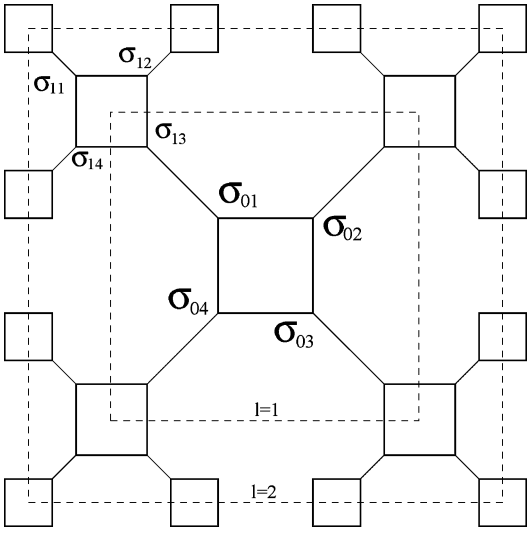

Figure 2. Square water on the Bethe lattice (quasichemical approximation). Each site of an usual Bethe lattice is placed by a square with four Ising spins on the vertexes.[27] Square water states are identified by Ising spins $\sigma = \pm 1$ ($\sigma = 1$ denotes the presence of the hydrogen atom, while $\sigma = -1$ indicates its absence), and solute particles are associated with four spins $\sigma = 0$. Sites of the same generation are linked by dashed lines ($l = 1$ and $l = 2$). The central generation is identified by $l = 0$.

3.1. Pure Square Water. Consider a Cayley tree of coordination four and replace the usual tree sites with squares (see Figure 2). Water states (Figure 1a) are identified through spin variables σ at the vertexes of the square ($\sigma = 1$ denotes the presence of a hydrogen atom, while $\sigma = -1$ indicates its absence). According to the "ice rule" for neutrality,[22] the sum of the four Ising spins at the vertexes of a square must vanish. The full partition function is given by:

$$Z(T) = \sum_{\{\sigma_{0i} = \pm 1\}} \delta_{\xi,0}\, g_0(\sigma_{01}) g_0(\sigma_{02}) g_0(\sigma_{03}) g_0(\sigma_{04}) \qquad (1)$$

where $\xi = \sum_{i=1}^{4} \sigma_{0i}$ and the first subindex of the Ising spin identifies the tree generation, and the second one identifies the particular branch (see Figure 2). $g_l(\sigma_{li})$ is the partition function of the ith branch of generation l ($l = 0, 1, ..., L$). The neutrality condition represented by the Kronecker delta yields a very simple form for the partition function (eq 1)

$$Z(T) = 6 g_0^{\,2}(+) g_0^{\,2}(-) \qquad (2)$$

Defining $R_l = g_l(-)/g_l(+)$, the recursion relations on the tree are given by

$$R_l = \frac{e^{1/t} R_{l-1} + 1}{R_{l-1} + e^{1/t}}$$

where $t = k_B T/\epsilon$. For $L \to \infty$, the fixed point solution converges to $R = 1$, and using the Gujrati prescription,[27,47] it is possible to write the free energy per particle for pure square water as:

$$-\beta f = \ln\left[\frac{3}{2}(e^{1/t} + 1)^2\right]$$

For the specific heat, we have:

$$\frac{C}{k_B} = \frac{2\, e^{-1/t}}{t^2 (e^{-1/t} + 1)^2} \qquad (3)$$

which is free of singularities. Note that an independent bond approximation for square water on a Bravais lattice, with $Z_N = (1 + e^{1/t})^{2N}$ for two states per bond, discussed by Nadler and Krausch,[24] leads to the same expression for the specific heat.

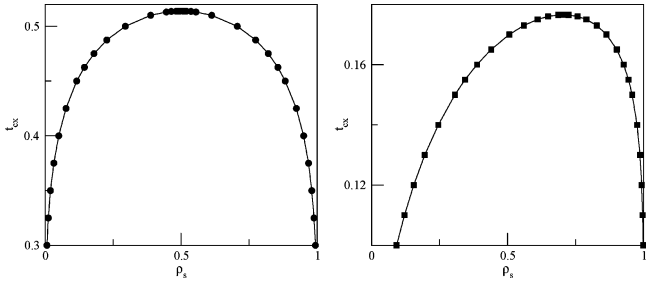

Figure 3. Temperature−concentration phase diagram, as a function of solute density ρ_s, for the aqueous solution of nonpolar (left) and polar solutes (right), from calculations on the Bethe lattice. In the case of polar solutes, the parameters are $v = 1.1$, $u = 0$, and $s = 0.5$. The critical temperatures are, respectively, $t_c^{\text{cayley}} = 1/ln(7) = 0.51389$ (with critical concentration of 0.500 ± 0.006) and $t_c^{\text{cayley}} = 0.17657$ (with critical concentration of 0.705 ± 0.004).

3.2. Square Water as a Solvent with Nonpolar Solutes. In the mixture, solutes are identified by four Ising spins $\sigma = 0$. In the grand canonical ensemble, the partition function is:

$$\Xi(T, \mu_a, \mu_s) = 6\, e^{\beta\mu_w} g_0^{\,2}(+) g_0^{\,2}(-) + e^{\beta\mu_s} g_0^{\,4}(0)$$

where μ_w (μ_s) is the water (solute) chemical potential. Defining

$$x_l \equiv \frac{g_l(0)}{g_l(+)}, \qquad y_l \equiv \frac{g_l(0)}{g_l(-)} \qquad (4)$$

the recursion relations for the branch partition functions $g_l(\sigma)$ may be written as

$$x_l = \frac{1 + 3z(x_{l-1}^{-2} y_{l-1}^{-1} + x_{l-1}^{-1} y_{l-1}^{-2})}{1 + 3z(e^{1/t} x_{l-1}^{-2} y_{l-1}^{-1} + x_{l-1}^{-1} y_{l-1}^{-2})}$$

$$y_l = \frac{1 + 3z(x_{l-1}^{-2} y_{l-1}^{-1} + x_{l-1}^{-1} y_{l-1}^{-2})}{1 + 3z(x_{l-1}^{-2} y_{l-1}^{-1} + e^{1/t} x_{l-1}^{-1} y_{l-1}^{-2})} \qquad (5)$$

where $z \equiv e^{\beta\mu}$ is the activity, and $\mu \equiv \mu_w - \mu_s$. To obtain the temperature−concentration phase diagram, we look at the density of water particles ($\rho \equiv \rho_{\text{water}}$) at the central site of the tree:

$$\rho(T, \mu) = \frac{6z}{6z + x_0^{\,2} y_0^{\,2}} \qquad (6)$$

Equation 6 gives us a relation between the water density ρ and the activity z:

$$3z = \gamma (x_0 y_0)^2 \qquad (7)$$

with $\gamma \equiv (\rho/2(1 - \rho))$. Recursion relations (eq 5) may be rewritten as functions of the density and gain much simpler form. In the thermodynamic limit, they yield the following equations for the fixed point:[48]

$$x = \frac{\gamma(x + y) + 1}{\gamma(x + e^{1/t} y) + 1}$$

$$y = \frac{\gamma(x + y) + 1}{\gamma(y + e^{1/t} x) + 1} \qquad (8)$$

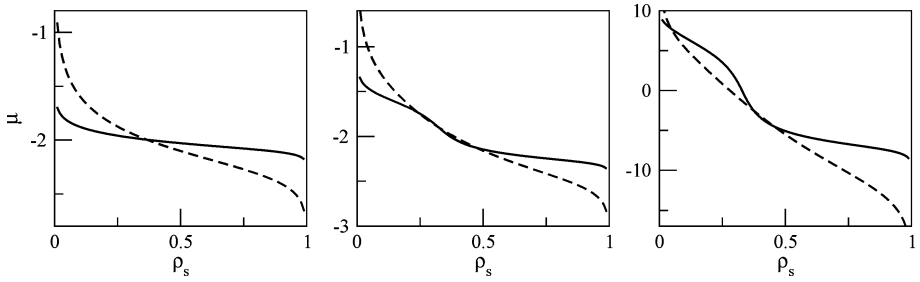

Figure 4. Chemical potential vs solute density ρ_s at the central site for symmetric van der Waals interactions $u = s = 0$. Left panel: $v = 1.01$ ($t = 0.1$ and $t = 0.025$). Central panel: $v = 1.1$ ($t = 0.025$ and $t = 0.1$). Right panel: $v = 3.0$ ($t = 0.4$ and $t = 2$). Lower temperatures correspond to the continuous lines and higher temperatures to dashed lines.

Under the physical conditions on the ratio of partitions functions, $x \geq 0$ and $y \geq 0$, we have:

$$x = y = \frac{2\gamma - 1 + \sqrt{(1-2\gamma)^2 + 4\gamma(1+e^{1/t})}}{2\gamma(1+e^{1/t})} \qquad (9)$$

leading, through (eq 7), to

$$\mu(\rho, t) = \epsilon t\left\{4\ln\left[\frac{2\rho-1}{1-\rho} + \sqrt{\left(\frac{2\rho-1}{1-\rho}\right)^2 + 2\frac{\rho}{1-\rho}(1+e^{1/t})}\right] - 4\ln(1+e^{(1/t)}) - \ln 6 - 3\ln\left(\frac{\rho}{1-\rho}\right)\right\} \qquad (10)$$

The chemical potential as function of density presents van der Waals loops, implying the existence of phase separation. Critical temperature is given by $t_c(\rho = 0.5) = 1/\ln(7)$. Maxwell construction yields the phase diagram presented in Figure 3, left.

3.3. Square Water as a Solvent with Polar Solutes. For polar solutes, the tree recursion relations at the fixed point are given by:

$$x = \frac{\gamma(x + e^{v/t}y) + e^{s/t}}{\gamma\, e^{u/t}(x + e^{1/t}y) + 1}$$

$$y = \frac{\gamma(x + e^{v/t}y) + e^{s/t}}{\gamma\, e^{u/t}(e^{1/t}x + 1) + e^{v/t}}$$

with $v \equiv \delta/\epsilon$, $u \equiv (v_{ww} - v_{ws})/\epsilon$, and $s \equiv (v_{ss} - v_{ws})/\epsilon$. The parameter v is a measure of the importance of solute−water hydrogen bonding with respect to water−water HBs. Parameters u and s introduce asymmetry in the van der Waals interaction.

If we consider van der Waals interactions that favor phase separation of solute ($s = 0.5$ and $u = 0$) and solute−solvent HBs that favor the mixture ($v = 1.1$), the system presents the temperature−concentration phase diagram shown in Figure 3, right. The competition between the two kinds of interactions introduces an asymmetry on the phase diagram, as compared to the case of the nonpolar solution (Figure 3, left). Note also that the critical temperature is correspondingly lowered.

The choice of $v > 1$ favors the mixture of water and polar solutes at low temperatures through hydrogen bonding. For $v = 1.01$, $v = 1.1$, and $v = 3.0$, and symmetric van der Waals interactions ($u = s = 0$), loops in the chemical potential are absent, as expected. Note, however, the unusual behavior for $v = 1.1$ and $v = 3.0$, shown in Figure 4.

4. Monte Carlo Simulations

Monte Carlo simulations of the three models were carried out in the canonical ensemble. Two types of movement are needed. For the pure system, a new state is obtained using a local movement of the HB network: a water molecule is randomly chosen and a new state is randomly selected. In the case of the mixtures, an additional movement is introduced, which consists of a random distance exchange[49] between water and solute particles (a global movement). The state of the water molecule in its new position is chosen randomly. In all cases, the Metropolis probability is used.[50] Random numbers are generated from ran2.[51]

4.1. Square Water with Nonpolar Solutes. *4.1.1. Phase Separation.* In Figure 5, we present the behavior of the specific heat of the aqueous solution of nonpolar particles for different solute concentrations (from 10 to 90%) and several lattice sizes ($L = 10$, 20, 30, 60). The peak in the specific heat increases with lattice size, an indication of the presence of phase separation.

The temperature−concentration phase diagram was obtained from extrapolation to infinite lattice size of temperature for the specific heat maxima and is shown in Figure 6.

Differently from the Bethe result (Figure 3, left), the phase diagram obtained from simulations is slightly asymmetric: concentrations such as 10% and 90% (or 20% and 80%), for example, do not coexist at the same temperature. A similar feature, albeit much more pronounced, is found by Besseling and Lyklema[33] for a three-dimensional model with "ice model" hydrogen bonds. Curiously, in the case of the two-dimensional (2-D) model with no hydrogen entropy,[34,36] the asymmetry is in the "wrong" direction. It may thus possibly be attributed to the specificity of the orientational and/or to the hydrogen entropy on the bond network.

A technical point which arises from our studies is the difference in the symmetry of the temperature−concentration phase diagram as derived from Bethe or Monte Carlo calculations (compare Figures 3, left, and 6, right). This result confirms an interesting theoretical question: the representation of the model on the Cayley tree leads to a loss of orientational information, as already pointed out by Izmailian at al.[27] and confirmed in a previous work.[31]

4.1.2. Hydration Shell. We have suggested in an earlier paper[26] that the square water model might be able to mimic solute hydration. We showed that bond density of the first hydration shell was less sensitive to temperature than bulk hydrogen bonds.

In this study, we compare energy correlations of the solvation shell and of bulk water both for associating (square water) and van der Waals (usual lattice gas) solvents. Energy correlations are defined as $c_\alpha = \langle e_\alpha^2\rangle - \langle e_\alpha\rangle^2$ with $\alpha = s, a$, where the

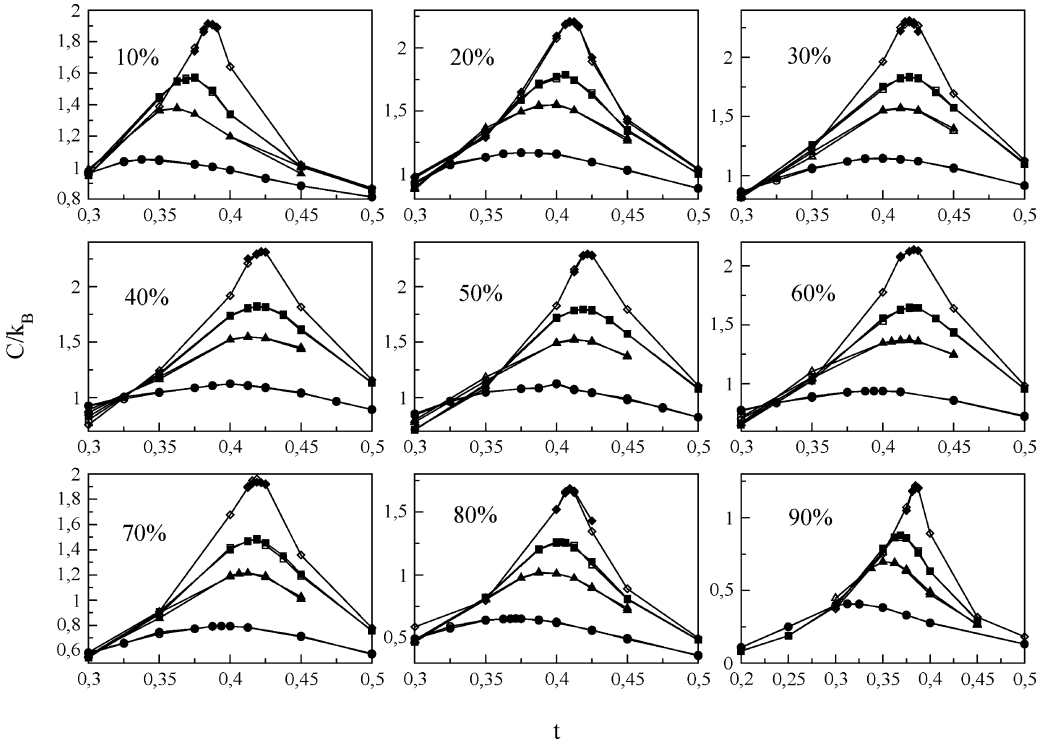

Figure 5. Specific heat for aqueous solution with nonpolar solutes for different solute concentrations: from 10 to 90%, as indicated on the figures. Empty end full symbols represent ordered and disordered initial conditions. Circles, triangles, squares, and diamonds correspond to $L = 10$, 20, 30, and 60 Monte Carlo results, respectively. The behavior as a function of system size indicates the presence of phase transition in all concentrations.

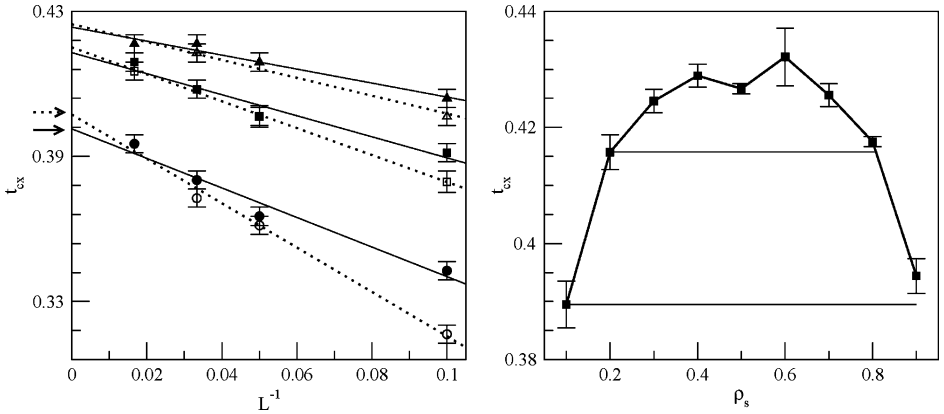

Figure 6. Left: temperature of maximum of specific heat as a function of inverse lattice size ($L = 10$, 20, 30, 60) for some solute concentrations (10, 20, and 30%: empty circles, squares, and triangles; 70, 80, and 90%: full triangles, squares and circles). Lines are extrapolations to $L \rightarrow \infty$. Note that symmetric pairs of concentrations (10−90, indicated by arrows, and 20−80) cross the temperature axis at different values, pointing to an asymmetry of the phase diagram. Right: temperature−concentration phase diagram as a function of solute density ρ_s, obtained from extrapolation to infinite size of data on the left. Tie lines indicate the coexistence temperature for concentrations of 10 and 20%. Note asymmetry quite far from the critical point (concentrations 10−90 and 20−80, for example).

index *s* stands for first shell (solvent molecules first neighbor to solute molecules), and the index *a* stands for all solvent molecules (solvent molecules surrounded by solvent molecules and first shell molecules).

In Figure 7a−c, energy correlations of the first hydration shell (first neighbors of nonpolar particles) and of all solvent molecules as a function of simulation time (measured in units of MC steps) are shown. In the low-temperature (coexistence) region, water molecules from the first hydration shell present larger energy correlation times with respect to bulk water. At higher temperatures (above coexistence), this relation is inverted and bulk water correlation relaxation is slightly larger than for the first hydration shell.

A very different behavior is presented by the nonassociating van der Waals solvent model, as can be seen in Figure 7d−f. The first solvation shell presents slightly *smaller* energy relaxation times than bulk solvent molecules *both* in the low- and high-temperature regions.

4.2. Square Water with Polar Solutes. The model solution with polar solutes was studied for HB parameters v, which favor dissolution, $v > 1$, and for two sets of van der Waals parameters: symmetric interactions ($u = s = 0$), which favor dissolution, and a second set ($u = 0$, $s = 0.5$), which favor phase separation.

In Figure 8, we show the behavior of the specific heat for several concentrations (from 10 to 40%) and different lattice sizes for ideal van der Waals interactions ($u = s = 0$) and hydrogen bond energies that favor dissolution ($v = 1.01$ and $v = 1.1$). For the higher value of v, two peaks independent of

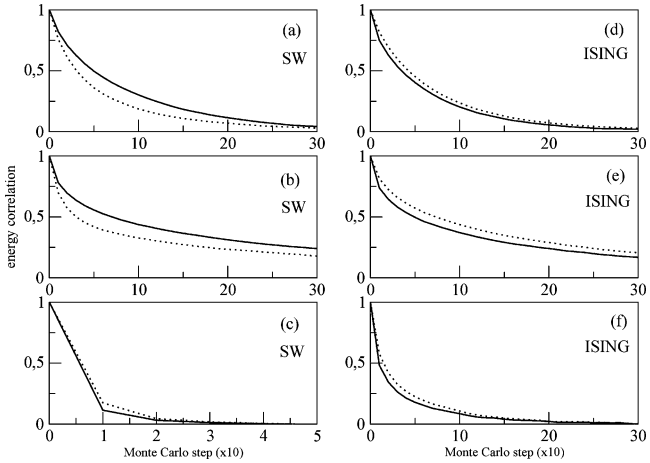

Figure 7. Energy correlations vs "time" (measured in units of MC steps) for the square water (SW) model (parts a, b, and c) and for the nonassociating (ISING) model (parts d, e, and f). Dashed lines correspond to energy correlations of all solvent molecules (hydration + bulk) and continuous lines to energy correlations of molecules in the first solvation shell. Correlations are shown for different temperature regimes: (a), (b), and (c): SW at $t/t_{cx} = 0.77$, 1.0, and 1.16; (d), (e), and (f): ISING at $t/t_{cx} = 0.8$, 1.0, and 1.1. Note that, at low temperatures, the opposite behavior of bulk and solvation water as compared to the nonassociating solvent. The two solvents have comparable behavior at higher temperatures. Concentration is at 10% and lattice size is $L = 60$ in both cases.

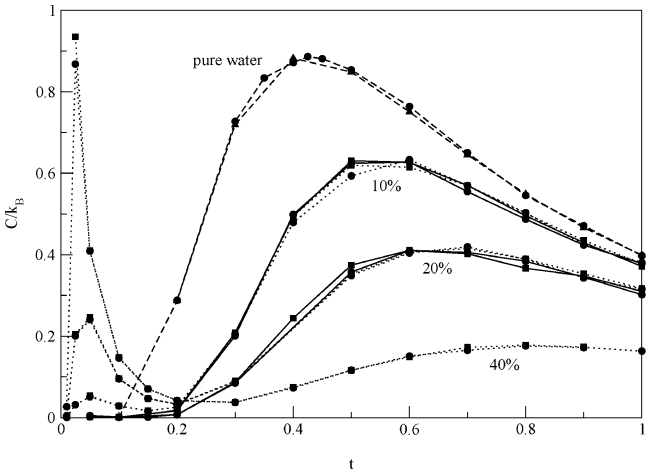

Figure 8. Specific heat for aqueous solution of polar solutes with symmetric van der Waals interactions, $u = s = 0$, for $v = 1.01$ (continuous line) and $v = 1.1$ (dashed line). Pure square water (long dashed line) is showed for illustration. Different solute concentrations are presented: 40, 20, and 10%, as indicated on the figure. Circles, triangles, and squares correspond to $L = 10$, 30, 60 Monte Carlo results, respectively.

lattice size are present, whereas for lower v, the low-temperature peak disappears.

The peak at higher temperatures can be associated with the loss of order of the hydrogen bond network, as can be seen from comparison with the specific heat of pure square water. As the solute concentration decreases, this peak becomes sharper and the maximum moves to smaller temperatures, approaching the behavior of pure water.

As to the second peak, at lower temperatures, its position is independent of but its height increases with solute concentration. Given a solute concentration, its height also diminishes as the parameter v, which controls the importance of solute−solvent HBs, is lowered, and disappears for small enough v, as in the case of $v = 1.01$. This suggests that it may be related to ordering

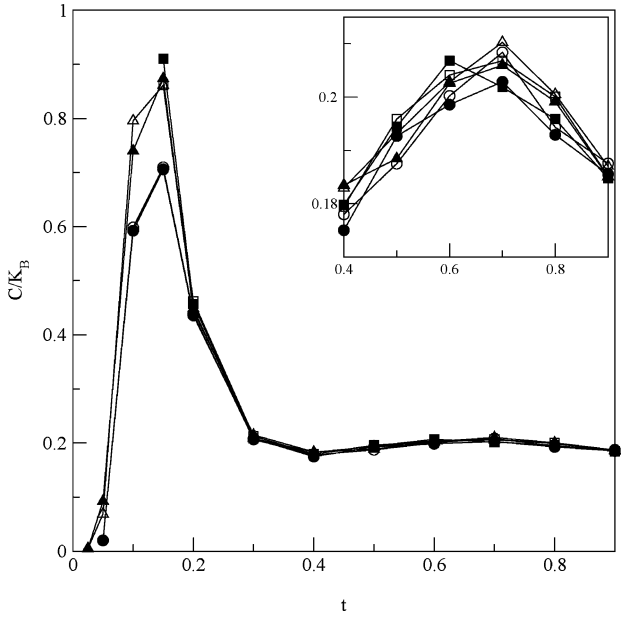

Figure 9. Specific heat for aqueous solution of polar solutes with $v = 1.1$, $u = 0$, and $s = 0.5$ and solute concentration of 40%. Circles, triangles, and squares correspond to $L = 10$, 30, 60 Monte Carlo results, respectively. Empty end full symbols represent ordered and disordered initial conditions. In the set we show the peak of high temperatures.

of the mixture. Note that the unusual behavior of the chemical potential found in calculations on the Bethe lattice (Figure 4) also is enhanced as v increases.

Phase coexistence is present in spite of favorable solute−solvent HBs, for $v = 1.1$, in the case of favorable van der Waals mixing parameters, $u = 0$ and $s = 0.5$, as seen in Figure 9 and in accordance with results found on the Bethe lattice (Figure 3, left). In Figure 9, specific heat also shows two peaks; however, in this case, the low-temperature peak is sensitive to lattice size, evidence of phase separation. The second peak is again related to loss of solvent order, as can be seen by inspection of Figures 8 and 9.

5. Conclusions

We have been able to establish a few properties of square water as solvent, which can be interpreted as consequences of the features characteristic of hydrogen bonding included in the model.

In the first place, the model exhibits enhanced structure of the first hydration shell. Parts a and b of Figure 7 show clearly that relaxation times for bonds in the first shell are longer than those of bulk water. Because the nonpolar noninteracting solute does not make hydrogen bonds, if one considers energy, then water in its first shell is likely to exchange this position in order to undertake a bulk water position in which it makes a larger number of bonds (maximum of four instead of a maximum of three). Thus, the behavior of the model would be the opposite of what we get, indicating that entropy, and not energy, is the main ingredient here. This argument gains weight from the fact that the van der Waals (nonassociating) solvent model, in which the entropy of bonds is absent, presents opposite behavior compared with square water (see Figure 7d and e). Taken together, the low sensitivity to temperature of the solvation shell as compared to that of bulk particles reported previously for square water[26] and the behavior of correlations presented here are strong evidence that the model presents hydrophobic hydration. The first hydration shell is more ordered, in agreement with some experimental results[8] and molecular dynamics

simulations,[12−15] which indicate enhancement of water structure on dissolution of nonpolar molecules. In summary, we have been able to probe a hitherto undisclosed microscopic feature of hydrophobic hydration. In previous related work on water solubility based on statistical models that take into account the directionality of bonding,[39−42] evidence of hydration has been obtained through the analysis of solvation thermodynamics, that is, entropy, enthalpy, and specific heat of solvation, whereas we focus on a dynamic property, namely the relaxation time for the solvation layer.

Second, our results indicate that the model might present a homogeneous low-temperature phase. Although not common, binary mixtures of water and hydrogen-bonding solutes may present both upper and lower critical temperatures, giving rise to closed loops of immiscibility.[52] Related theoretical studies[20,21] indicate that holes seem to be essential in order to have closed loops. On the other hand, ordering of the mixture at low temperatures is also a necessary feature for a lower consolute point to be present. The lower temperature peak in Figure 8 indicates that square water in the presence of polar solutes presents an ordered mixed pseudophase at low temperatures. The possibility of closed loops upon the introduction of holes suggests further investigation of the model might be of interest.

The anomalous properties of water rely both on the presence of the hydrogen bond net as well as on the low density associated to the latter. The role of the third important feature, hydrogen entropy on the bond network, has not been clearly established despite of some recent attempts.[37,38,41] The local density reduction on bonding is absent in our two-dimensional model because square water lacks density variables associated to bonds. The low-density specific volume required for the arising of HB clusters could be introduced ad hoc, as in the case of Potts models,[53] and an anomalous density behavior can certainly be expected. Besseling and Lyklema[33] have used ice model states on a three-dimensional lattice and have shown that the model displays a qualitatively correct liquid−vapor phase diagram. Introduction of density variations is also possible on a two-dimensional lattice,[30,31] and the anomalous behavior is there.

In summary, our purpose was to investigate the specific role of the orientational interaction upon the solvent behavior, precisely in the absence of the density feature. Some of the above results illustrate the utility of such an approach.

Acknowledgment. We thank B. Widom, who introduced us to the work of N. A. M. Besseling and J. Lyklema. We thank J. M. R. Enrique for fruitful discussions about water miscibility. We both acknowledge financial support from the Brazilian agency Fapesp.

References and Notes

(1) Franks, F., Ed. *Water: A Comprehensive Treatise*; Plenum Press: NY, 1972; Vol. 1−7. Franks, F., Ed. *Water Science Reviews*; Cambridge University Press: New York, 1985; Vol. 1−4.

(2) Pollack, G. L. *Science* **1991**, *251*, 1323.

(3) Atkins, P. W. *Physical Chemistry*, 4th ed.; Oxford University Press: New York, 1993.

(4) Widom, B.; Bhimalapuram P.; Koga, K. *Phys. Chem. Chem. Phys.* **2003**, *5*, 3085.

(5) Debenedetti, P. G. *Metastable Liquids*; Princeton University Press: Princeton, NJ, 1996.

(6) Frank, H. S.; Evans, M. W. *J. Chem. Phys.* **1945**, *13*, 507.

(7) Hidaka, F.; Kanno, H. *Chem. Phys. Lett.* **2003**, *379*, 216. Yui, H.; Kanoh, K.; Fujiwara, H.; Sawada, T. *J. Phys. Chem.* **2002**, *106*, 12041. Dixit, S.; Sopper, A. K.; Finney, J. L.; Crain, J. *Europhys. Lett.* **2002**, *59*, 377. Sopper, A. K.; Finney, J. L. *Phys. Rev. Lett.* **1993**, *71*, 4346.

(8) Hallenga, K.; Grigera, J. R.; Berendsen, H. J. C. *J. Phys. Chem.* **1980**, *84*, 2381.

(9) Hertz, H. G.; Zeidler, M. D. *Ber. Bunsen-Ges. Phys. Chem.* **1964**, *68*, 821.

(10) Turner, J.; Soper, A. *J. Chem. Phys.* **1994**, *101*, 6116.

(11) See refs 76−100 in Griffth, J. H.; Scheraga, H. A. *J. Mol. Struct. (THEOCHEM)* **2004**, *682*, 97; and refs 26−134 in Scheraga, H. A. *J. Biomol. Struct. Dyn.* **1998**, *16*, 447.

(12) Madan, B.; Sharp, K. *Biophys. Chem.* **1999**, *78*, 33.

(13) Guillot, B.; Guissani, Y. *J. Chem. Phys.* **1993**, *99*, 8075.

(14) Urahata S.; Canuto, S. *Chem. Phys. Lett.* **1999**, *313*, 235.

(15) Grigera, J. R.; Kalko, S. G.; Fischbarg, J. *Langmuir* **1996**, *12*, 154.

(16) Sastry, S.; Debenedetti, P. G.; Sciortino, F.; Stanley, H. E. *Phys. Rev. E* **1996**, *53*, 6144. Franzese, G.; Marques, M. I.; Stanley, H. E. *Phys. Rev. E* **2003**, *67*, 011103. Sastry, S.; Sciortino, F.; Stanley, H. E. *J. Chem. Phys.* **1993**, *98*, 9863.

(17) Roberts, C. J.; Debenedetti, P. G. *J. Chem. Phys.* **1996**, *105*, 658.

(18) Barkema, G. T.; Widom, B. *J. Chem. Phys.* **2000**, *113*, 2349. Kolomeisky, A. B.; Widom, B. *Faraday Discuss.* **1999**, *112*, 81.

(19) Widom, B. *Pol. J. Chem.* **2001**, *75*, 507.

(20) Lin, J. C.; Taylor, P. L. *Phys. Rev. Lett.* **1994**, *73*, 2863.

(21) Enrique, J. M. R.; Ponce, I. R.; Rull, L. F.; Marconi, U. M. B. *Phys. Chem. Chem. Phys.* **1999**, *1*, 4271.

(22) Lieb, E. H.; Wu, F. Y. Two-Dimensional Ferroelectric Models. In *Phase Transitions and Critical Phenomena*; Domb, C., Green, M. S., Ed.; Academic Press: New York, 1972; Vol. 1.

(23) Lieb, E. H. *Phys. Rev. Lett.* **1967**, *18*, 692.

(24) Nadler, W.; Krausche, T. *Phys. Rev. A* **1991**, *44*, R7888. Krausche, T.; Nadler, W. *J. Phys. B: At. Mol. Opt. Phys.* **1992**, *86*, 433.

(25) Attard, P.; Batchelor, M. T. *Chem. Phys. Lett.* **1988**, *149*, 206. Attard, P. *Physica A* **1996**, *233*, 742.

(26) Guisoni, N.; Henriques, V. B. *Braz. J. Phys.* **2000**, *30*, 736.

(27) Izmailian, N. Sh.; Hu, C. K.; Wu, F. Y. *J. Phys. A: Math. Gen.* **2000**, *33*, 2185.

(28) Soluble vertex models[22] are also derived from the ice model through the introduction of Boltzmann weights with possibly the addition of new (nonneutral) states, but the relation with the original physical basis for the ice model is lost.[26]

(29) Girardi, M.; Figueiredo, W. *J. Chem. Phys.* **2002**, *117*, 8926.

(30) Henriques, V. B.; Barbosa, M. C. *Phys. Rev. E* **2005**, *71*, 031504.

(31) Henriques, V. B.; Guisoni, N.; Barbosa, M. A.; Thielo, M.; Barbosa, M. C. *Mol. Phys.* **2005**, *103*, 3001.

(32) Bell, G. M. *J. Phys. C: Solid State Phys.* **1972**, *5*, 889. Lavis, D. A. *J. Phys. C: Solid State Phys.* **1973**, *6*, 1530.

(33) Besseling, N. A. M.; Lyklema, J. *J. Phys. Chem.* **1994**, *98*, 11610.

(34) Bell, G. M.; Lavis, D. A. *J. Phys. A: Gen. Phys.* **1970**, *3*, 568.

(35) Buzano, C.; De Stefanis, E.; Pelizzola, A.; Pretti, M. *Phys. Rev. E* **2004**, *69*, 061502.

(36) Patrykiejew, A.; Pizio, O.; Sokolowski, S. *Phys. Rev. Lett.* **1999**, *83*, 3442.

(37) Pretti, M.; Buzano, C. *J. Chem. Phys.* **2004**, *121*, 11856.

(38) Silverstein, K. A. T.; Haymet, A. D. J.; Dill, K. A. *J. Am. Chem. Soc.* **1998**, *120*, 3166. This is in fact a continuous version of the model proposed by Bell.[34]

(39) Besseling, N. A. M.; Lyklema, J. *J. Phys. Chem. B* **1997**, *101*, 7604.

(40) Eads, C. D. *J. Phys. Chem. B* **2002**, *106*, 12282.

(41) Pretti, M.; Buzano, C. *J. Chem. Phys.* **2005**, *123*, 024506.

(42) Xu, H.; Dill, K. A. *J. Phys. Chem. B* **2005**, *109*, 23611.

(43) To maintain a clear distinction between lattice bonds and hydrogen bonds, we have chosen to call the former lattice lines.

(44) Stillinger, F. H. *Science* **1980**, *209*, 451.

(45) Eisenbeg, D.; Kauzmann, W. *The Structure and Properties of Water*; Clarendon: Oxford, U.K., 1969.

(46) For a general vertex model, different weights may be attributed to each vertex state,[22,27] while for the square water model, the six possible states must have the same weight.

(47) Gujrati, P. D. *Phys. Rev. Lett.* **1995**, *74*, 809.

(48) Also, for the numerical treatment, it is interesting to obtain expressions as function of density because it is limited $0 \leq \rho \leq 1$.

(49) Shida, C.; Henriques, V. B. *Int. J. Mod. Phys. C* **2000**, *11*, 1.

(50) Metropolis, N.; Rosenbluth, A. W.; Rosenbluth, M. N.; Teller, A. H.; Teller, E. *J. Chem. Phys.* **1953**, *21*, 1087.

(51) Press, W. H.; Teukolsky, S. A.; Vetterling, W. T.; Flannery, B. P. *Numerical Recipes in C*, 2nd ed.; CambridgeUniversity Press: Cambridge, MA, 1998.

(52) Yalkowsky, S. H. *Solubility and Solutilization in Aqueous Media*, Oxford University Press: New York, 1999.

(53) Sastry, S.; Debenedetti, P. G.; Sciortino F.; Stanley, H. E. *Phys. Rev. E* **1996**, *53*, 6144. Franzese, G.; Marques, M. I.; Stanley, H. E. *Phys. Rev. E* **2003**, *67*, 011103.